Metrology of Optical Systems

Figures and Images for Instructors

Module 2

Non-Interferometric

Measurement of Optical Performance

Precision Optics Series

National Center for Optics and Photonics Education

This text was developed by the National Center for Optics and Photonics Education (OP-TEC), University of Central Florida, under NSF ATE grant 1303732. Any opinions, findings, and conclusions or recommendations expressed in this material are those of the author(s) and do not necessarily reflect the views of the National Science Foundation.

Published and distributed by
OP-TEC
University of Central Florida
http://www.op-tec.org

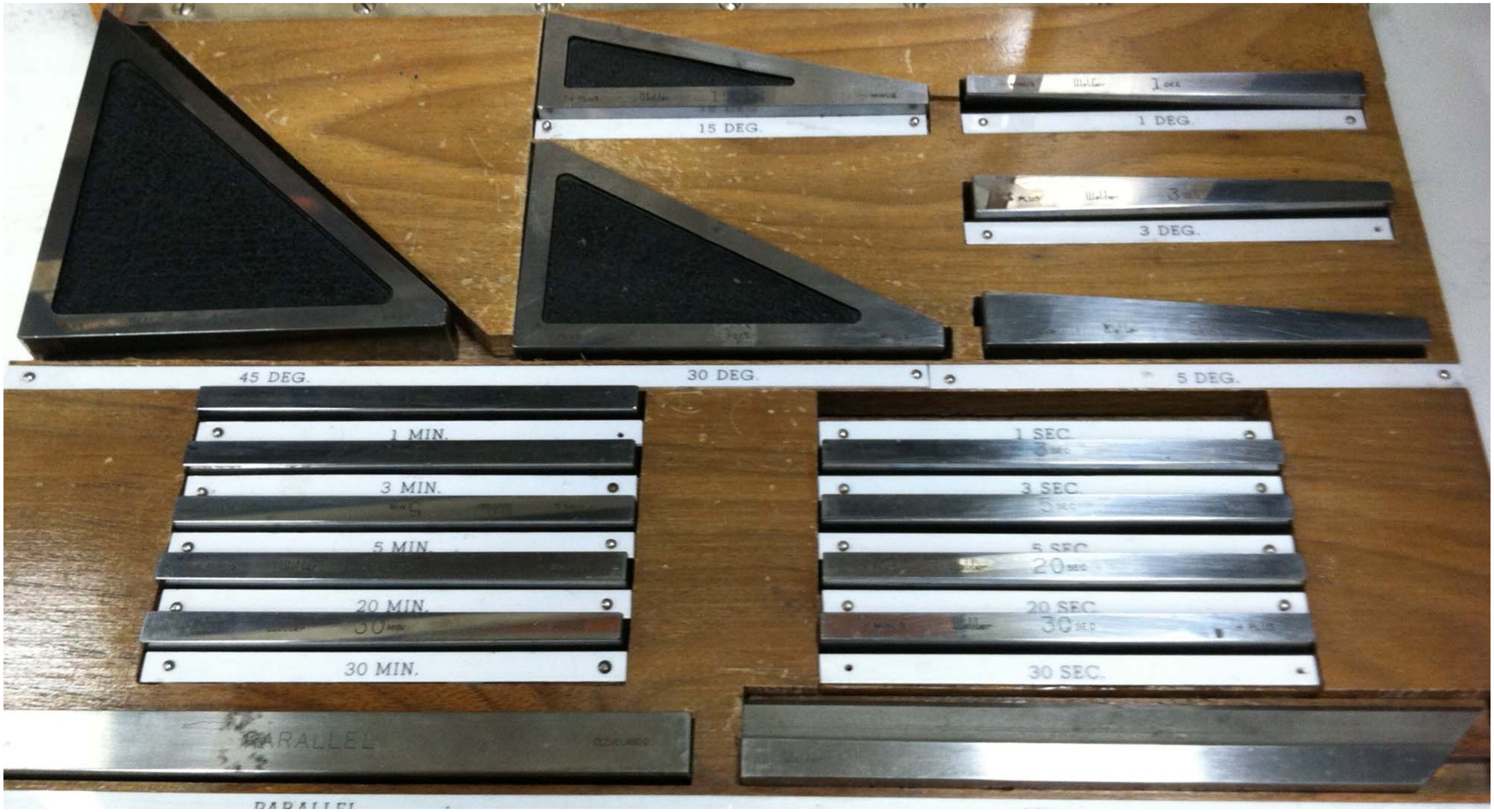

Figure 2-1 *In protective cases, precision physical distance and angle references called gauge blocks are shown here.*
(Photos courtesy Firas Almarzouk of Supply Chain Optics.)

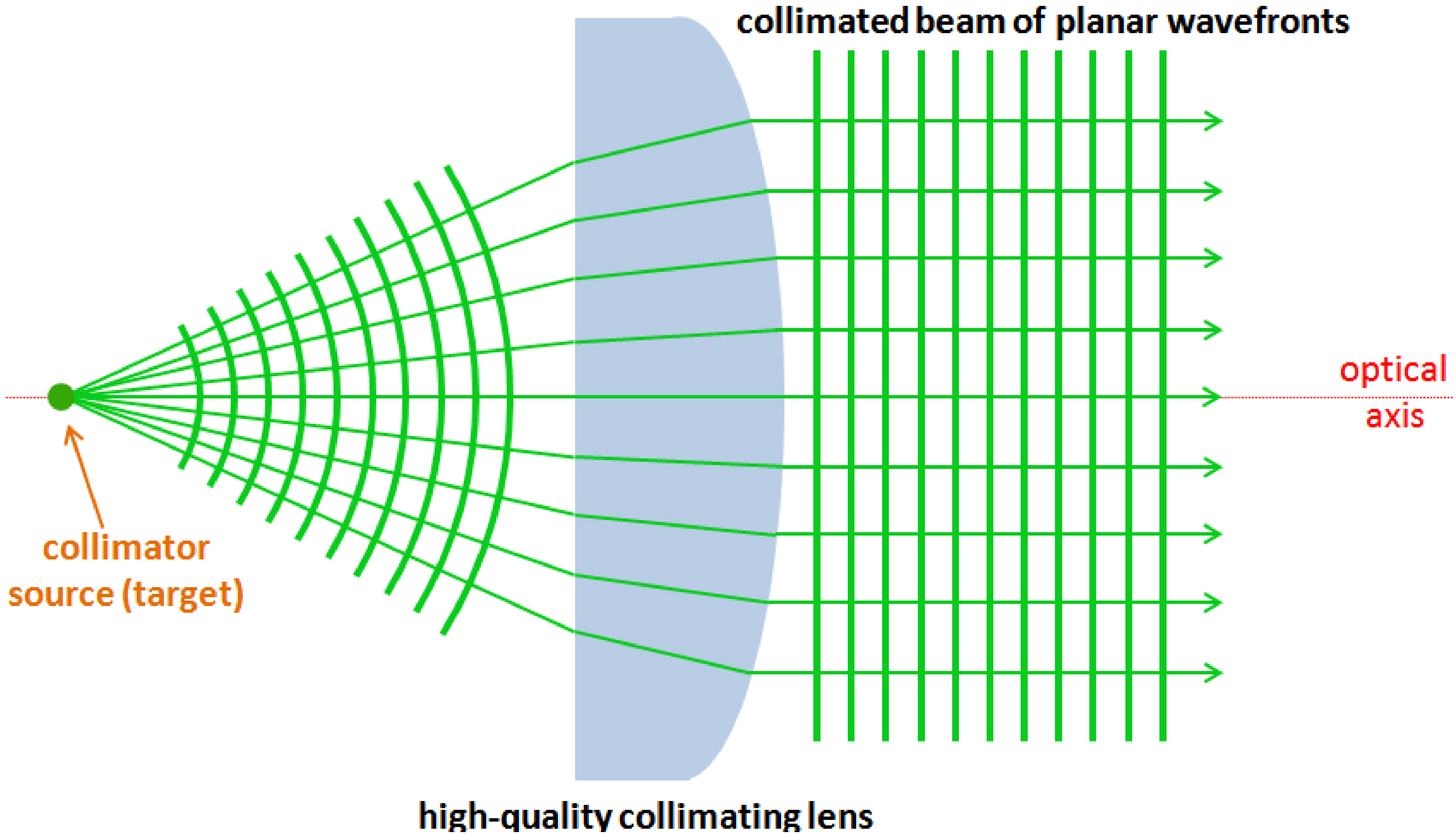

Figure 2-2 *A source of finite size, as given by the equation below, is collimated into a beam of planar wavefronts by the ideal lens that represents a well-corrected collimator*

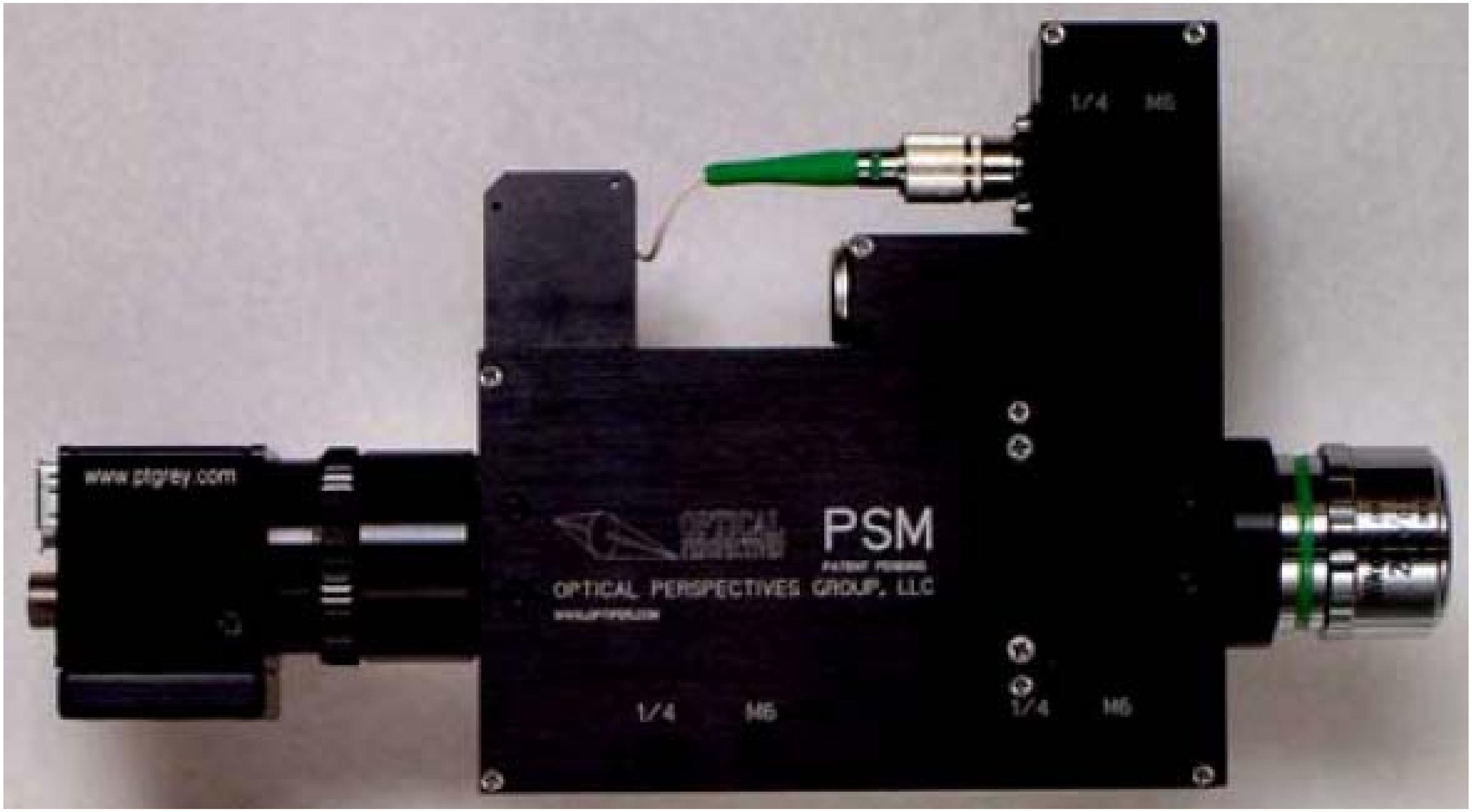

Figure 2-3 *The point-source microscope (PSM) is a valuable optical alignment tool acting as a point source for integration and alignment applications.*

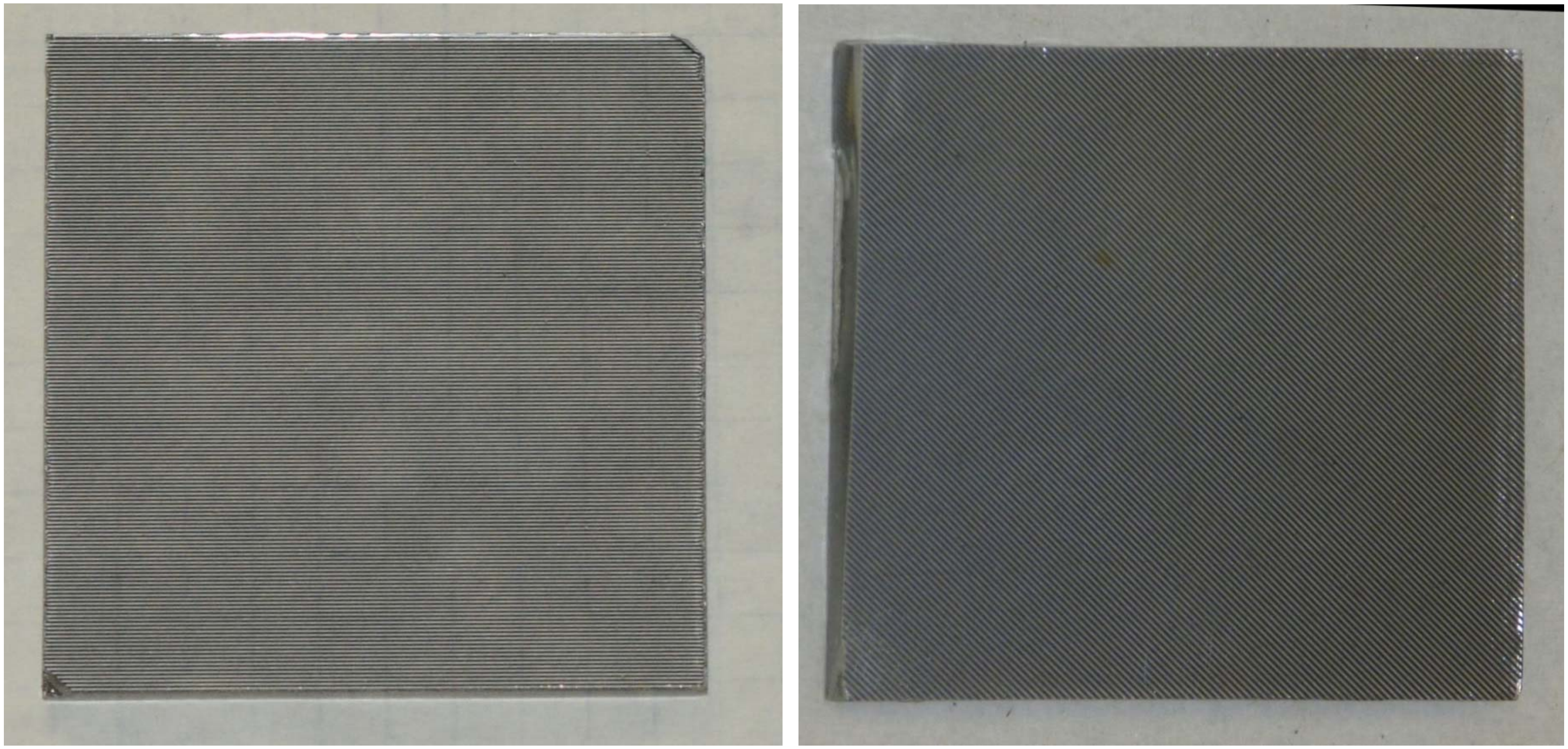

Figure 2-4 *Ronchi rulings like these are precision glass plates with periodically alternating transparent and opaque (or reflective and transmissive) regions. These Ronchi rulings have features at 3 and 4.7 lines per millimeter (l/mm), which may not be apparent if this image is rendered at a low resolution.*

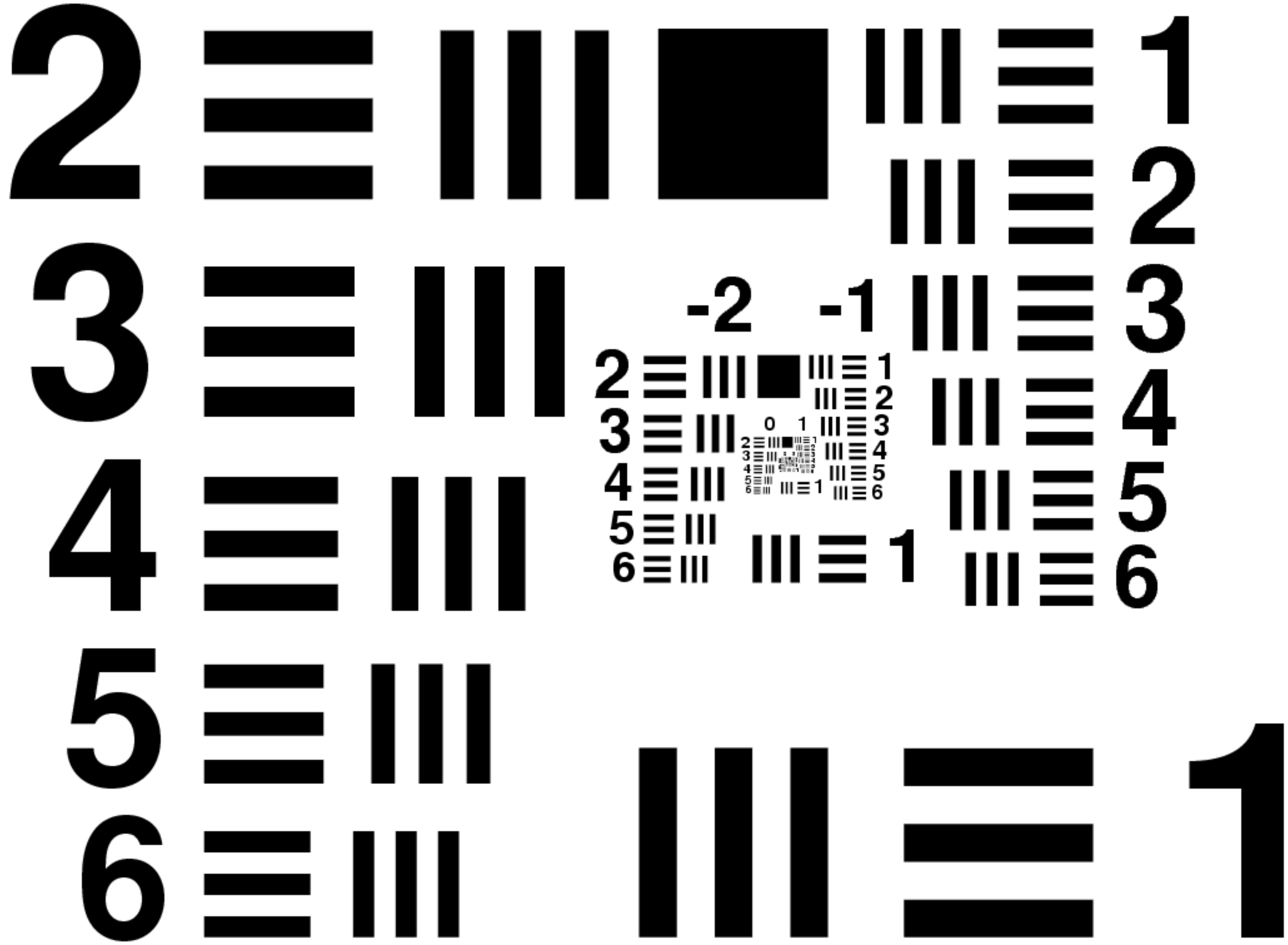

Figure 2-5 *The 1951 USAF Bar Chart: an array of Ronchi rulings is often used as the object or target during measurement of optical system parameters*

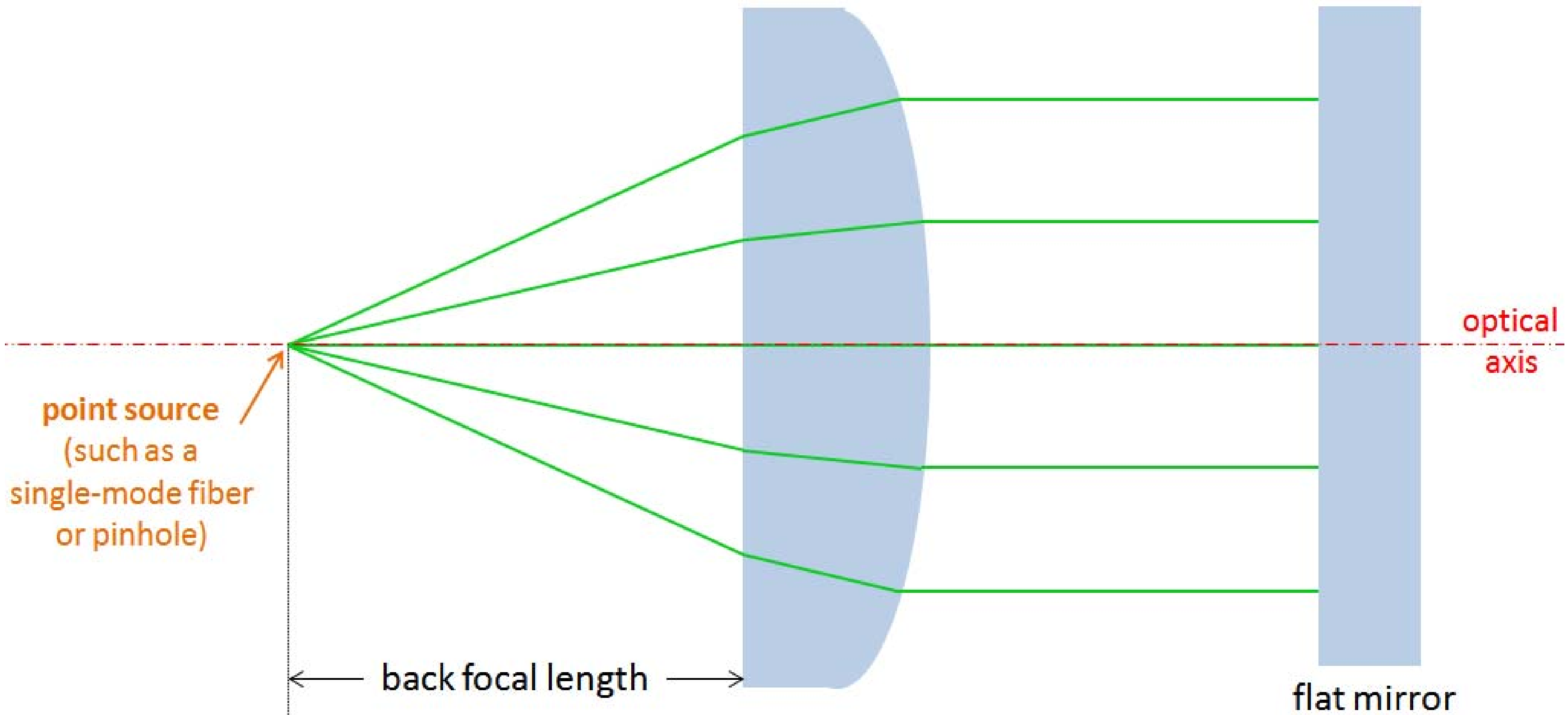

Figure 2-6 *This figure shows the autocollimation technique used to test an optical system with a positive focal length*

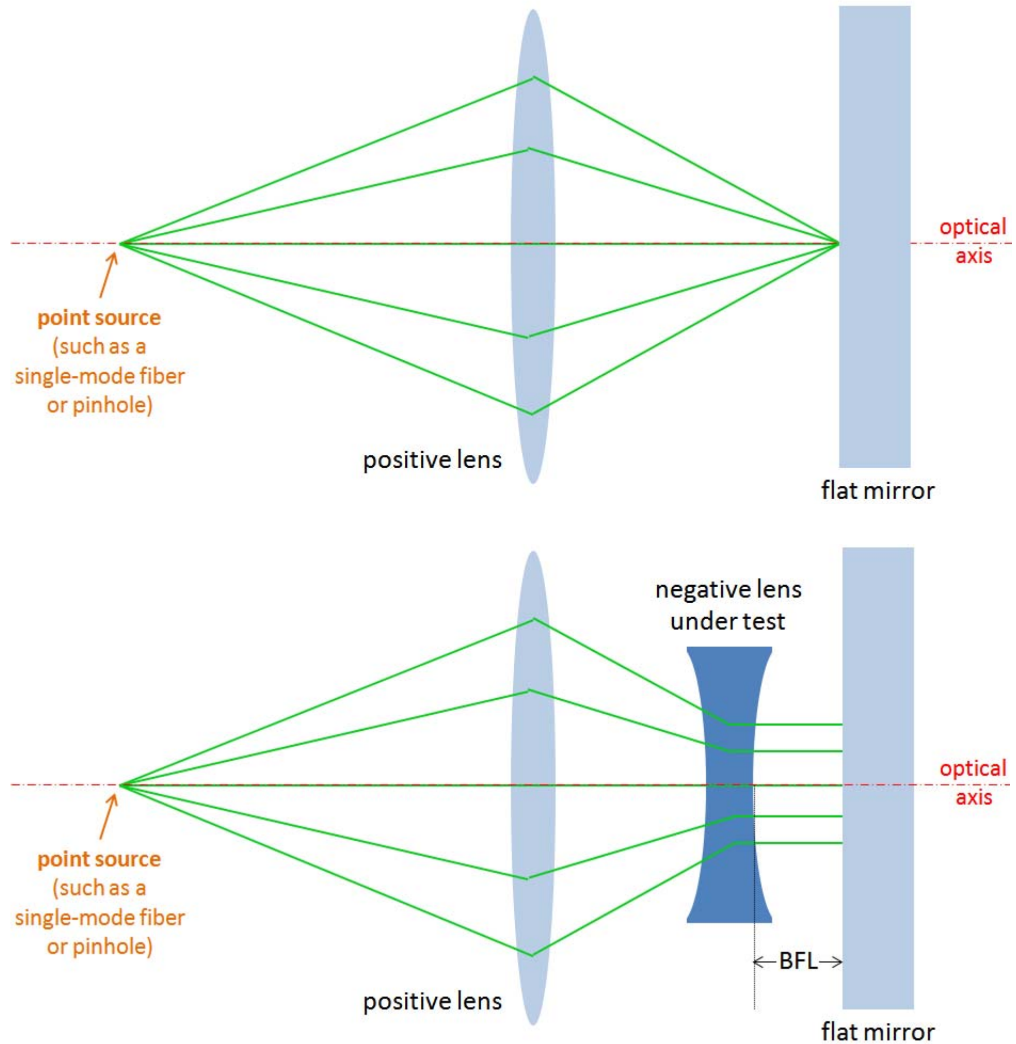

Figure 2-7 *This figure shows the autocollimation technique used to test an optical system with a negative focal length*

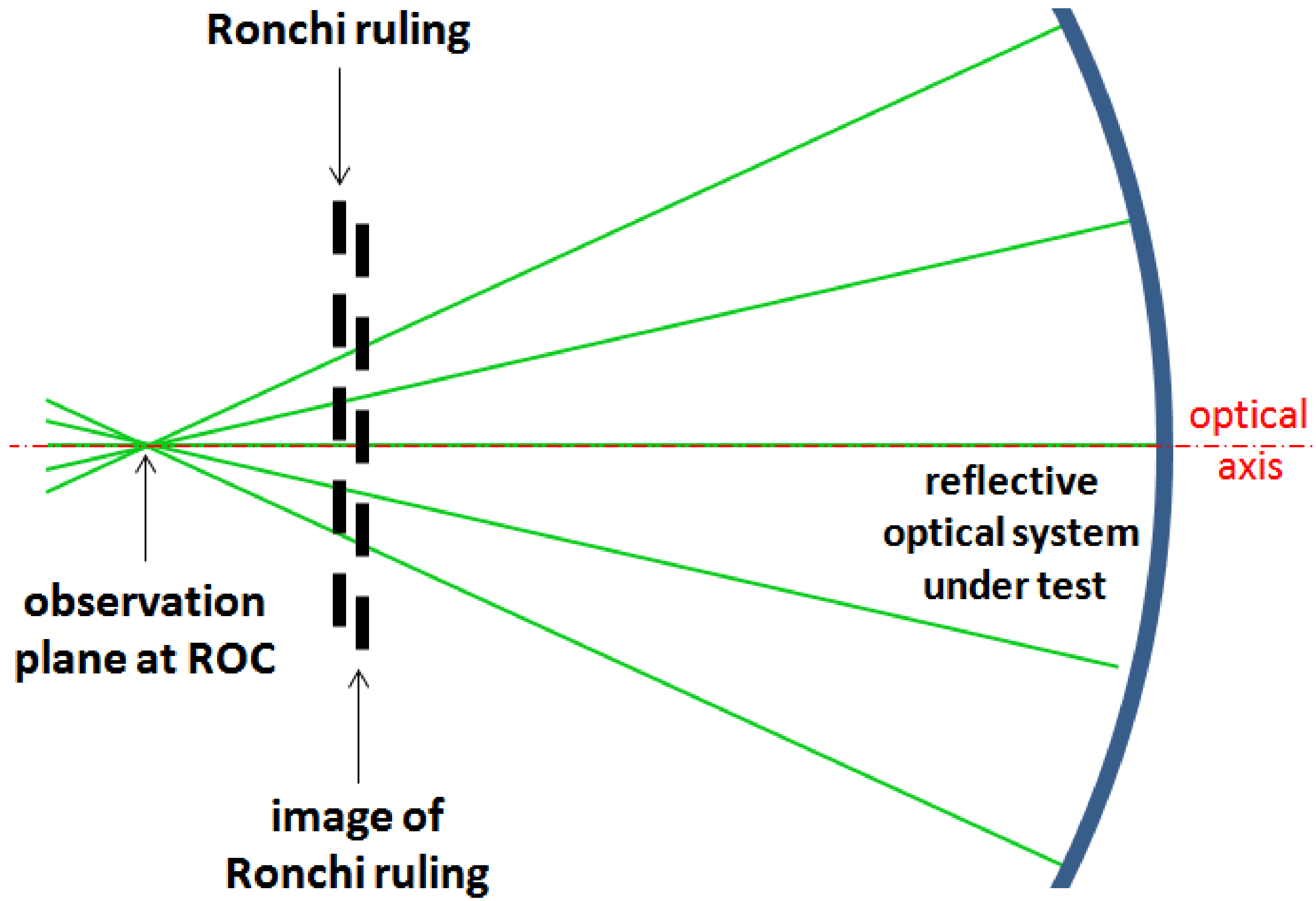

Figure 2-8 *This traditional Ronchi test configuration for a mirror.*

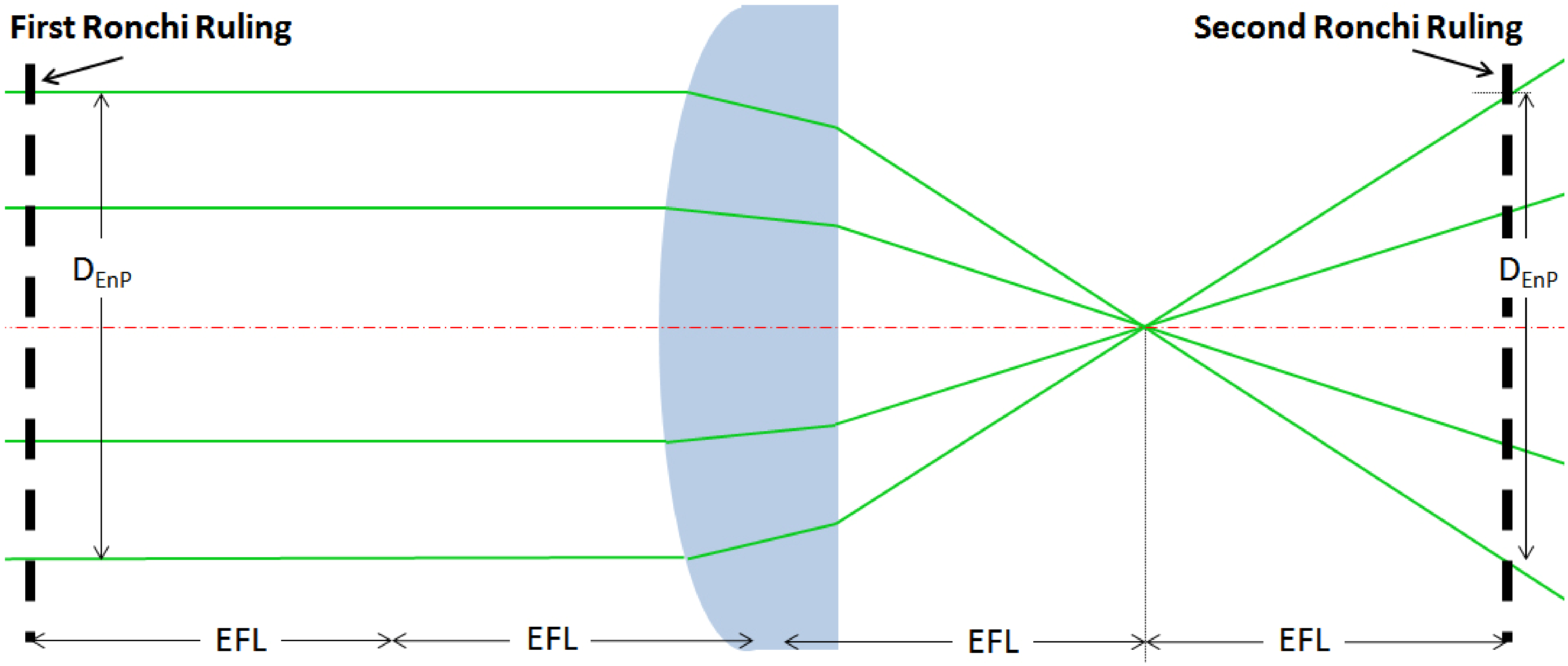

Figure 2-9 *This novel and robust test configuration, conceived by Malacara-Doblado, et al., uses Ronchi rulings to measure the EFL and other optical properties of an optical system.*

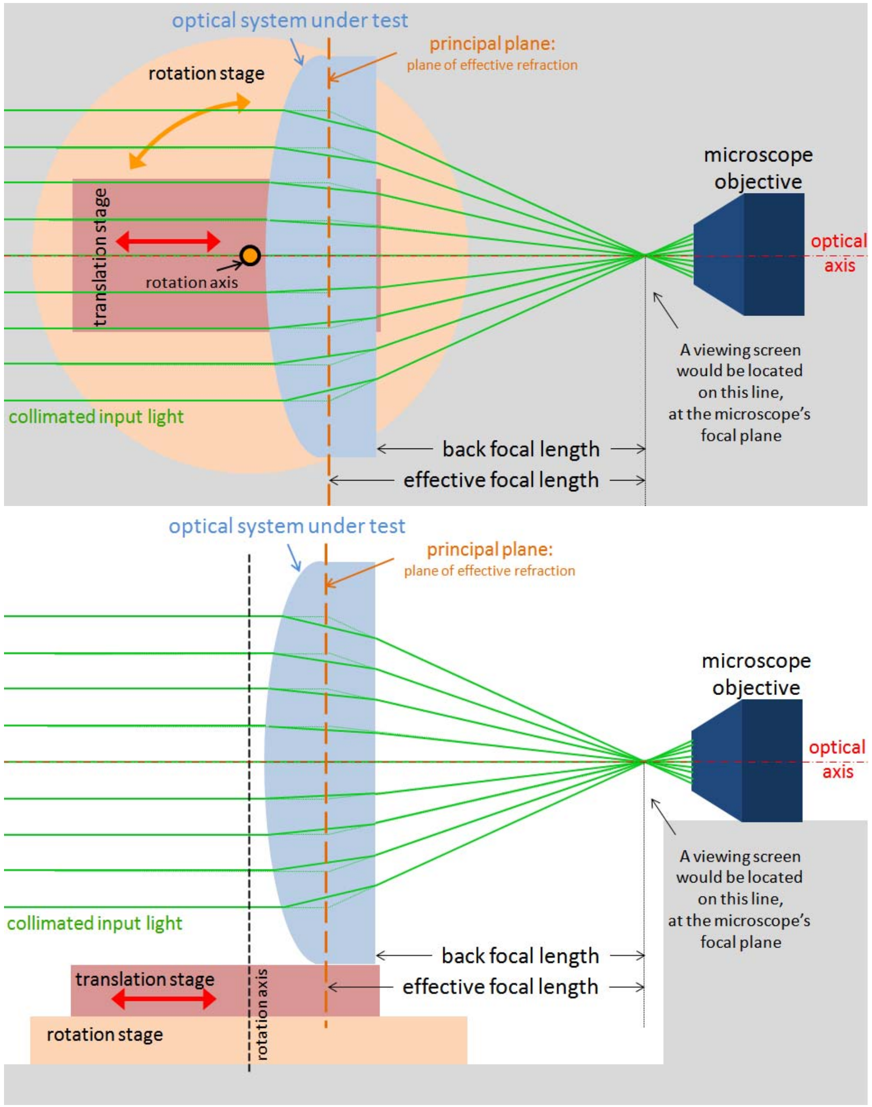

Figure 2-10 *This figure shows the plan and side view of a nodal slide with a microscope used to view the image in space—the finely dashed line represents the image plane that is viewed by the microscope or the plane at which a screen or sensor would be placed.*

Figure 2-11 *A focimeter like the optical instrument shown here might be used in an optometrist's office or at an eyeglass merchant. Its layout resembles a microscope in that the user looks in the eyepiece, and the eyeglass lens under test is inserted in the gap at the center of the instrument.*

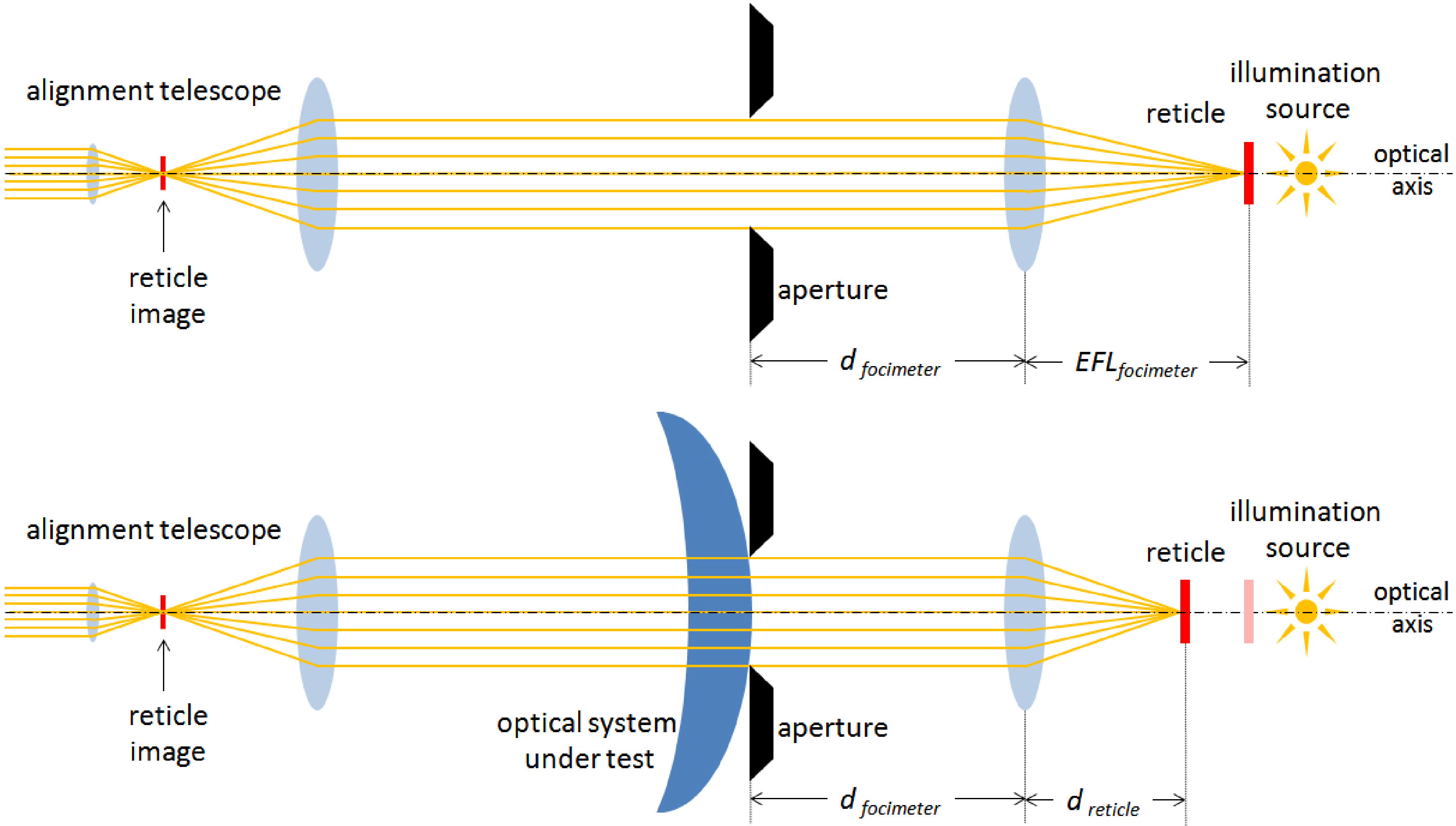

Figure 2-12 *This figure shows the operation of the focimeter without (top) and with (bottom) the optical system under test. The addition of the optical system under test moves the position of the reticle from* $EFL_{focimeter}$ *to* $d_{reticle}$*, thereby allowing calculation of the BFL for the optical system under test.*

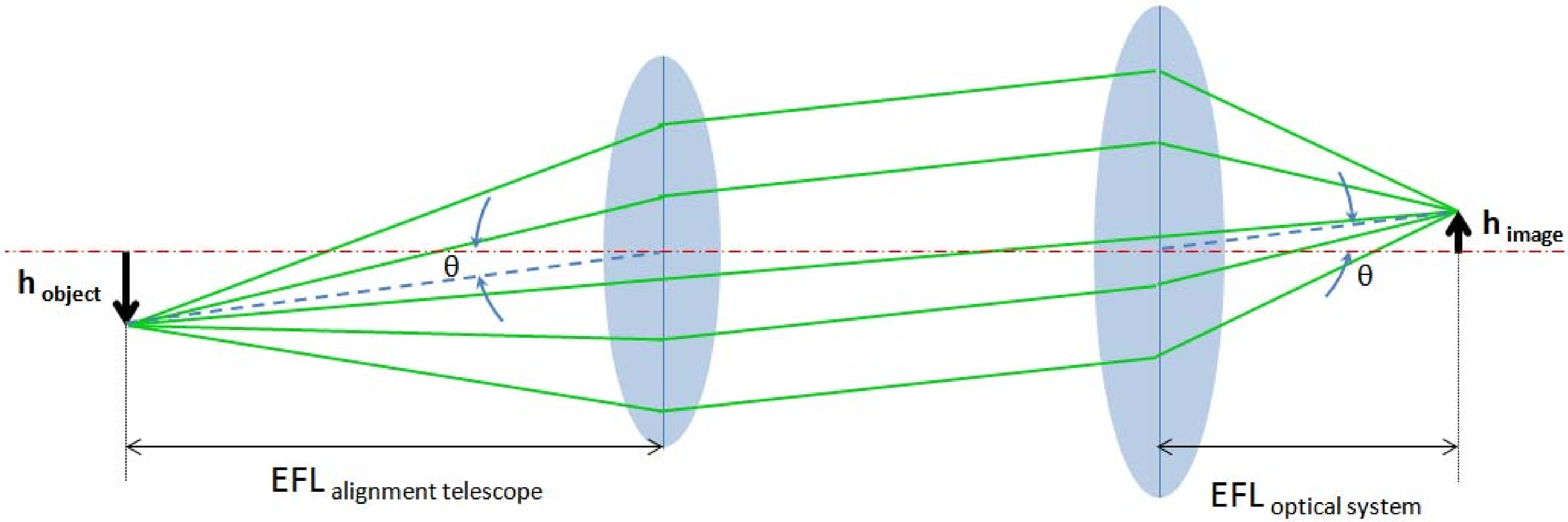

Figure 2-13 *Alignment telescope configured to image an object of size h_{object} to optical infinity*

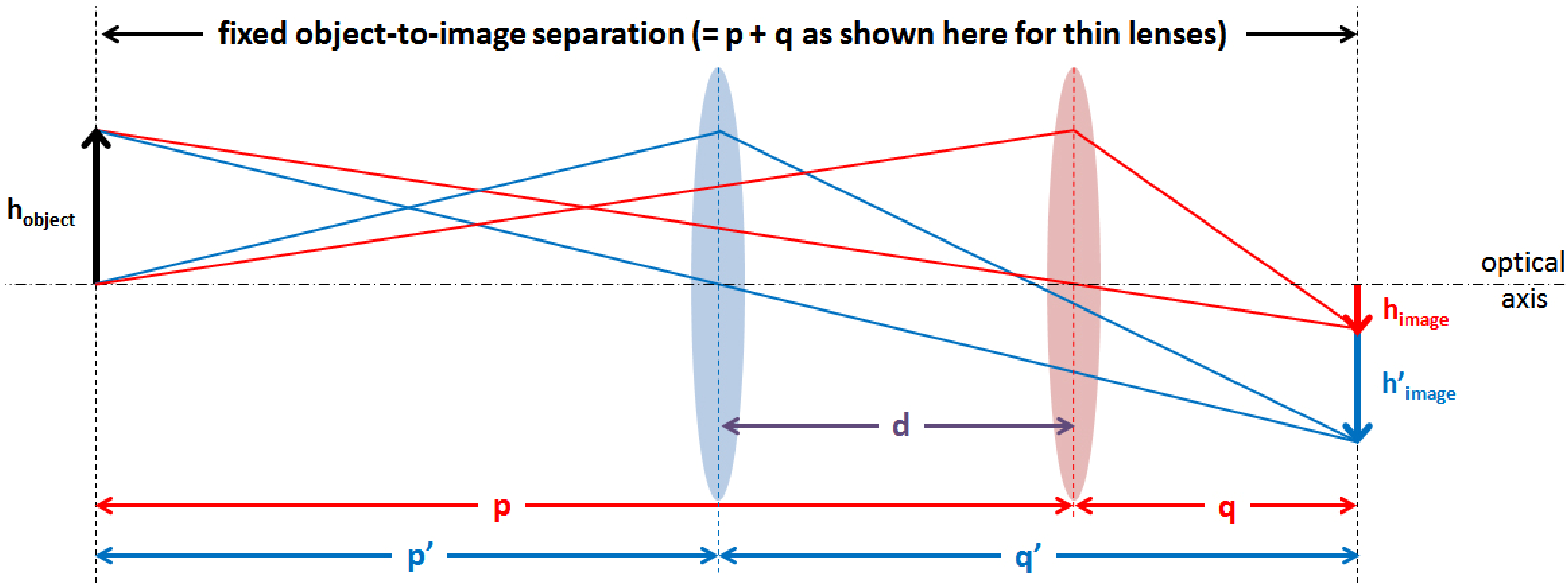

Figure 2-14 *For every fixed object-to-image separation, an optical system will form images at two different magnifications, depending on the location of the optical system between its object and image.*

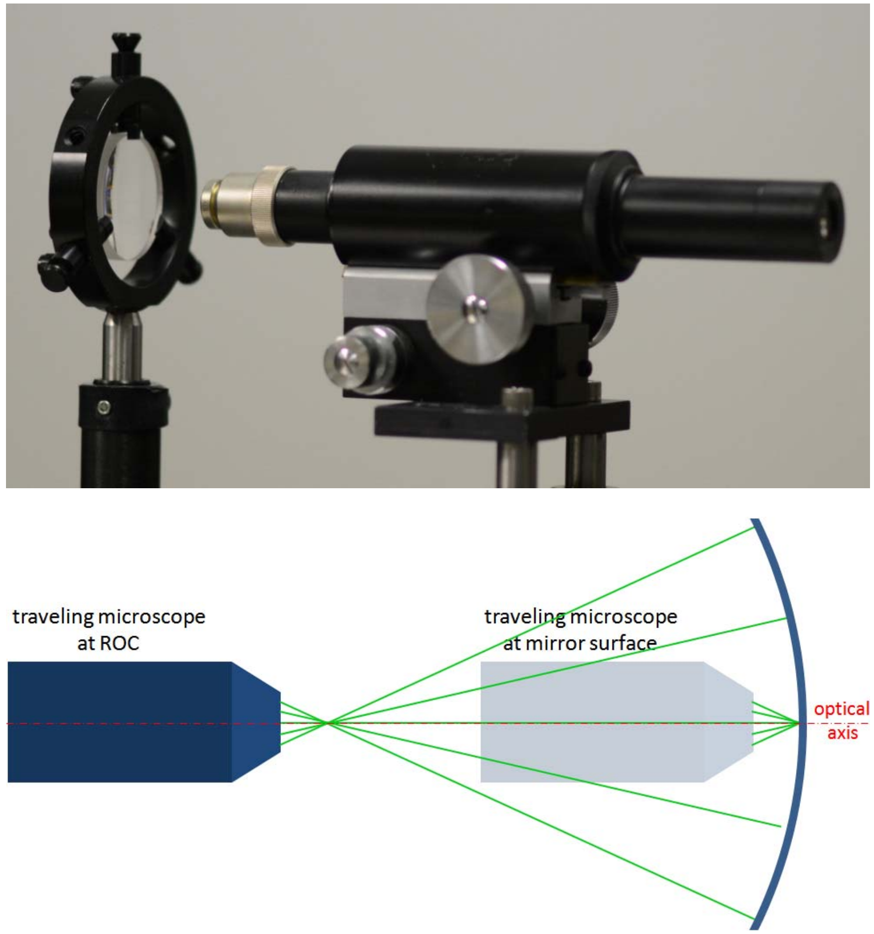

Figure 2-15 *The traveling microscope shown is focused on a lens surface. The microscope focuses on a point on an optic. It is focused in the schematic to a point on an optical surface in the right configuration, and at the surface's radius of curvature (ROC) in the left configuration.*

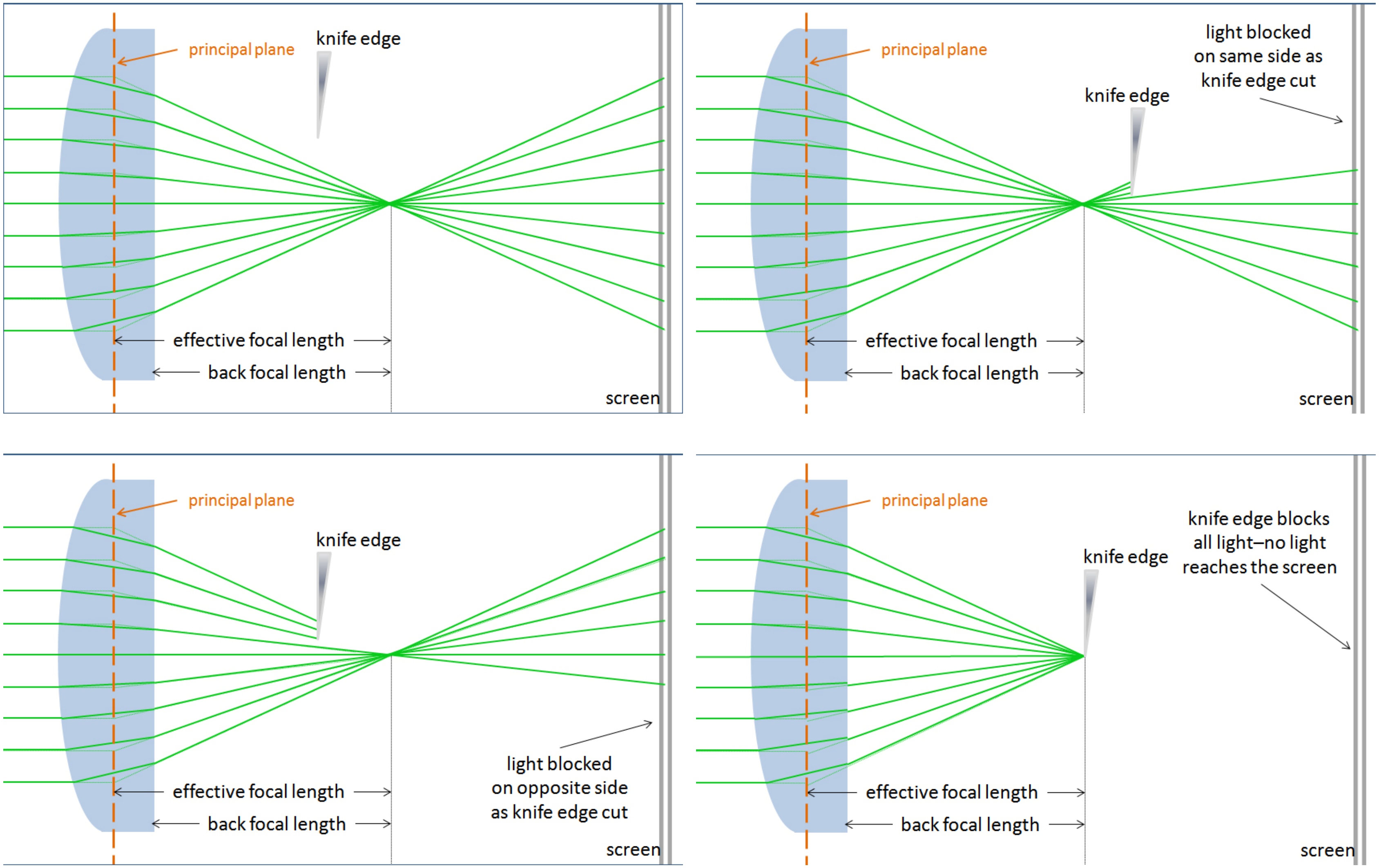

Figure 2-16 *The set up for the Foucault test is shown, illustrating the results that will be observed on a screen when the knife edge cuts the beam before, after, and at the focal point of the lens*

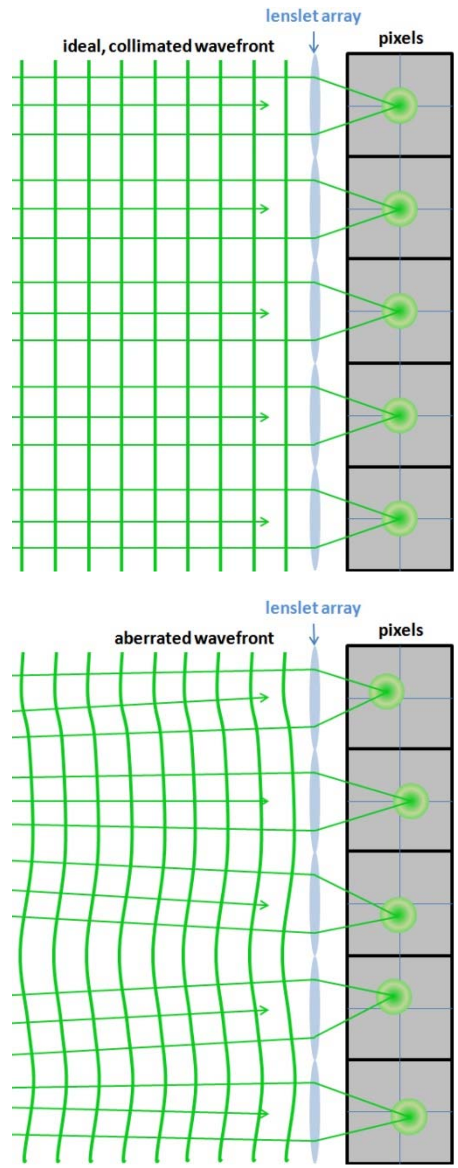

Figure 2-17 *These figures show (top) the ideal spot locations for a collimated, unaberrated plane wave, and (bottom) the spot locations for the different subaperture tilts of an aberrated wavefront in a Shack-Hartmann wavefront sensor configuration.*

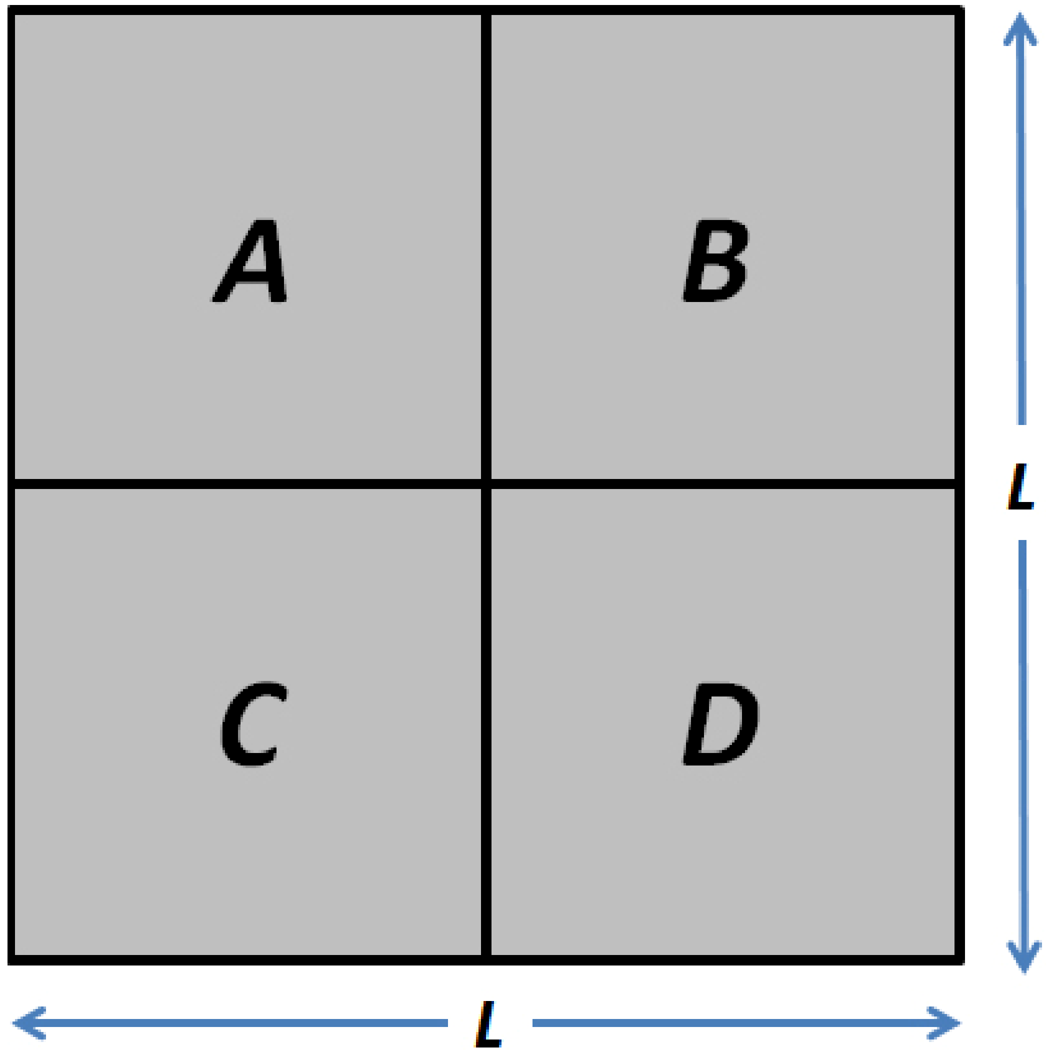

Figure 2-18 *Each of the four small squares represents a camera pixel. The transverse (x, y) location of a spot that illuminates this 2-by-2 pixel region will be determined by Equation 2-6, in which A, B, C, and D are the optical power values in each of the pixels.*

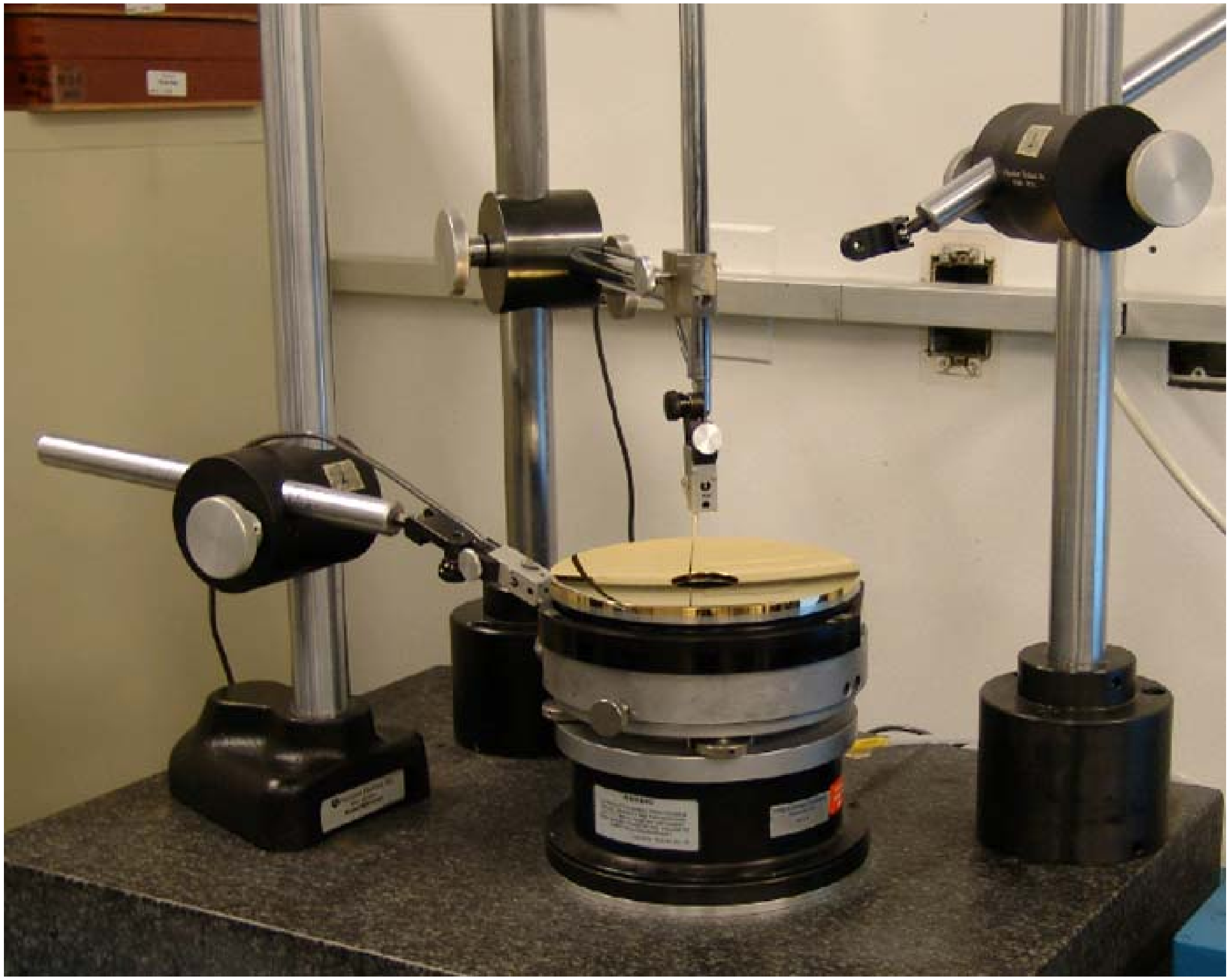

Figure 2-19 *The CMM shown in the figure is outfitted with multiple probes that measure the surface of the diamond-turned asphere. (Photo courtesy OPN.)*

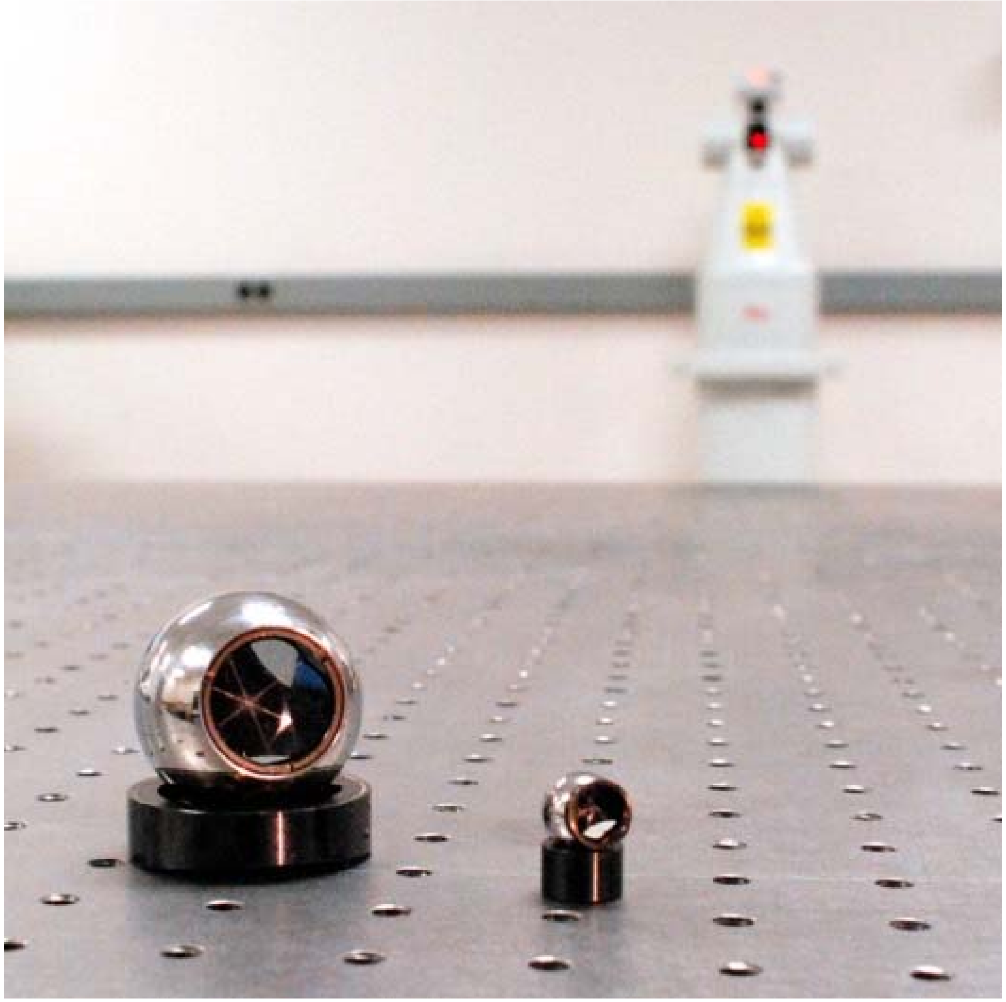

Figure 2-20 *A laser tracker is shown in the background on this image, and two SMRs are located on the optical breadboard in the foreground. (Photo courtesy OPN.)*

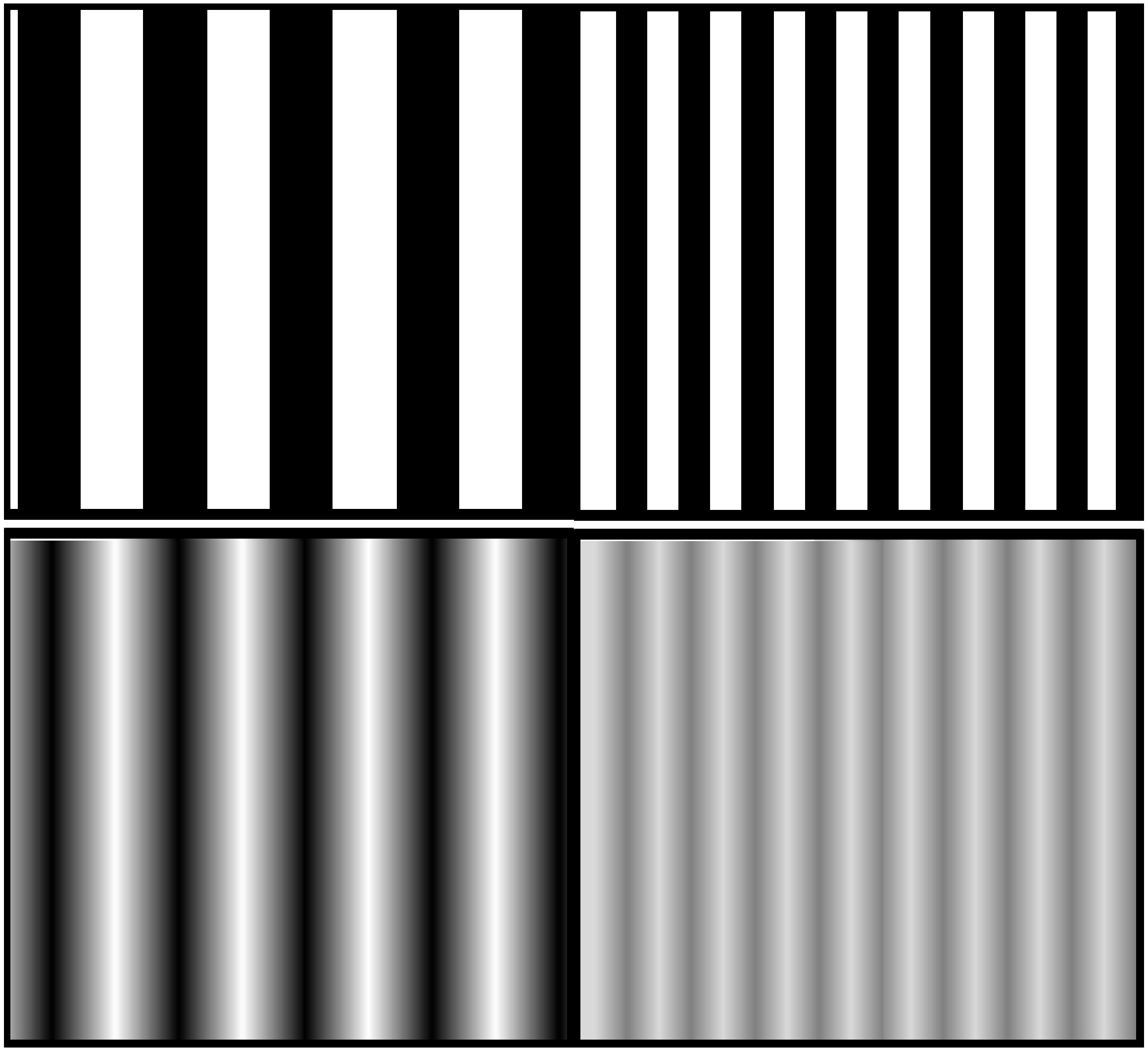

Figure 2-21 *These figures show how the contrast is more poorly imaged for objects with higher spatial frequency than for low-spatial-frequency objects.*

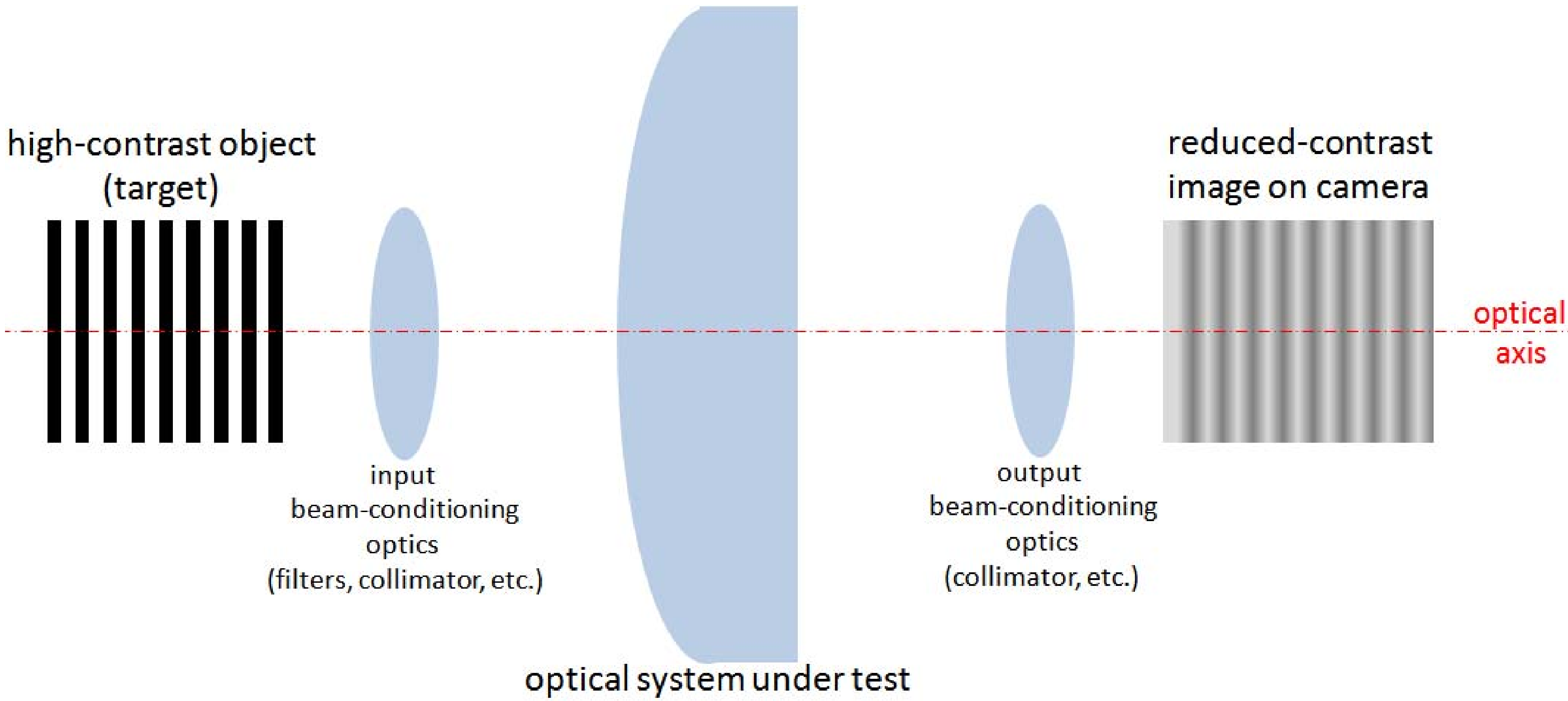

Figure 2-22 *Block diagram of an MTF-measurement system*

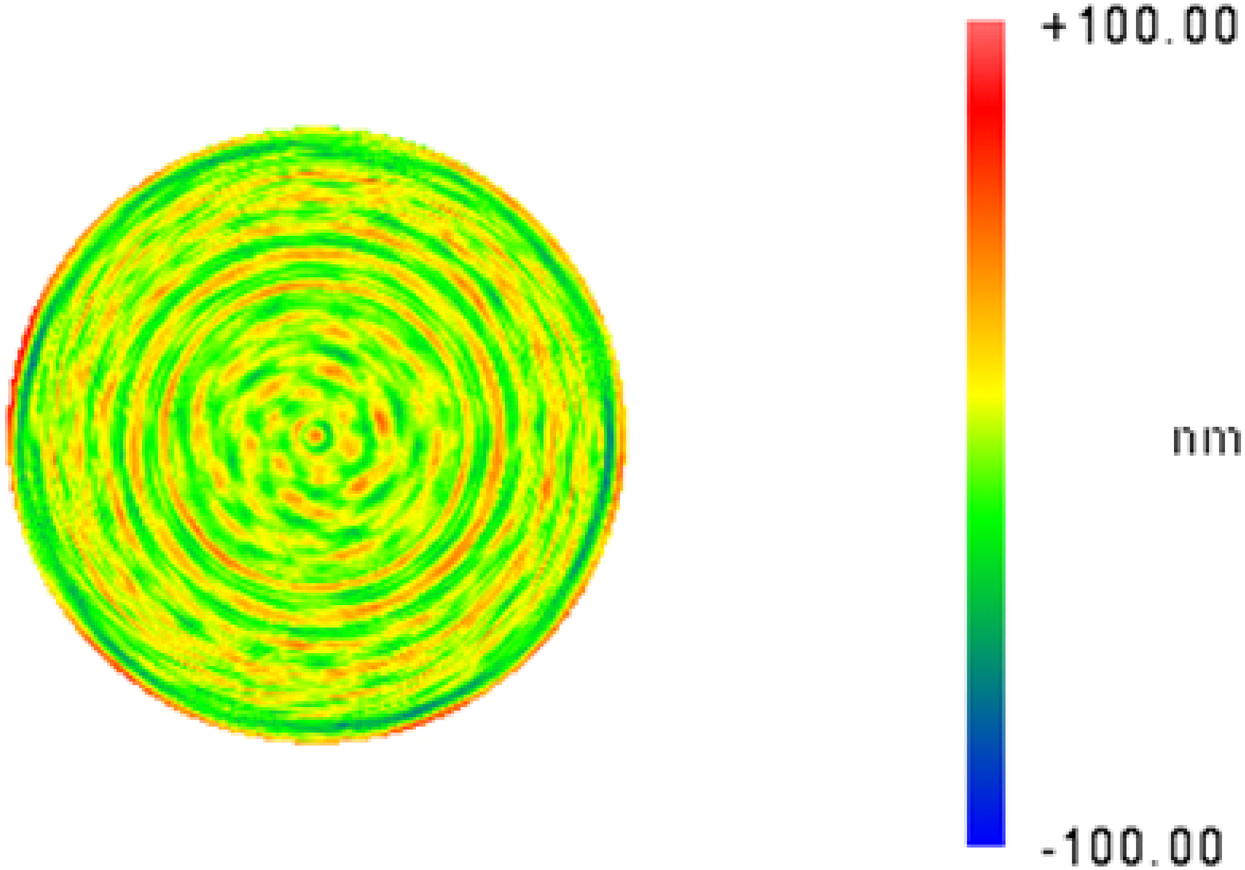

Figure 2-23 *Mid-spatial frequency error will manifest itself if ripples like those shown here are evident in an interferogram.*
(Courtesy R. Youngworth and U. Fuchs)

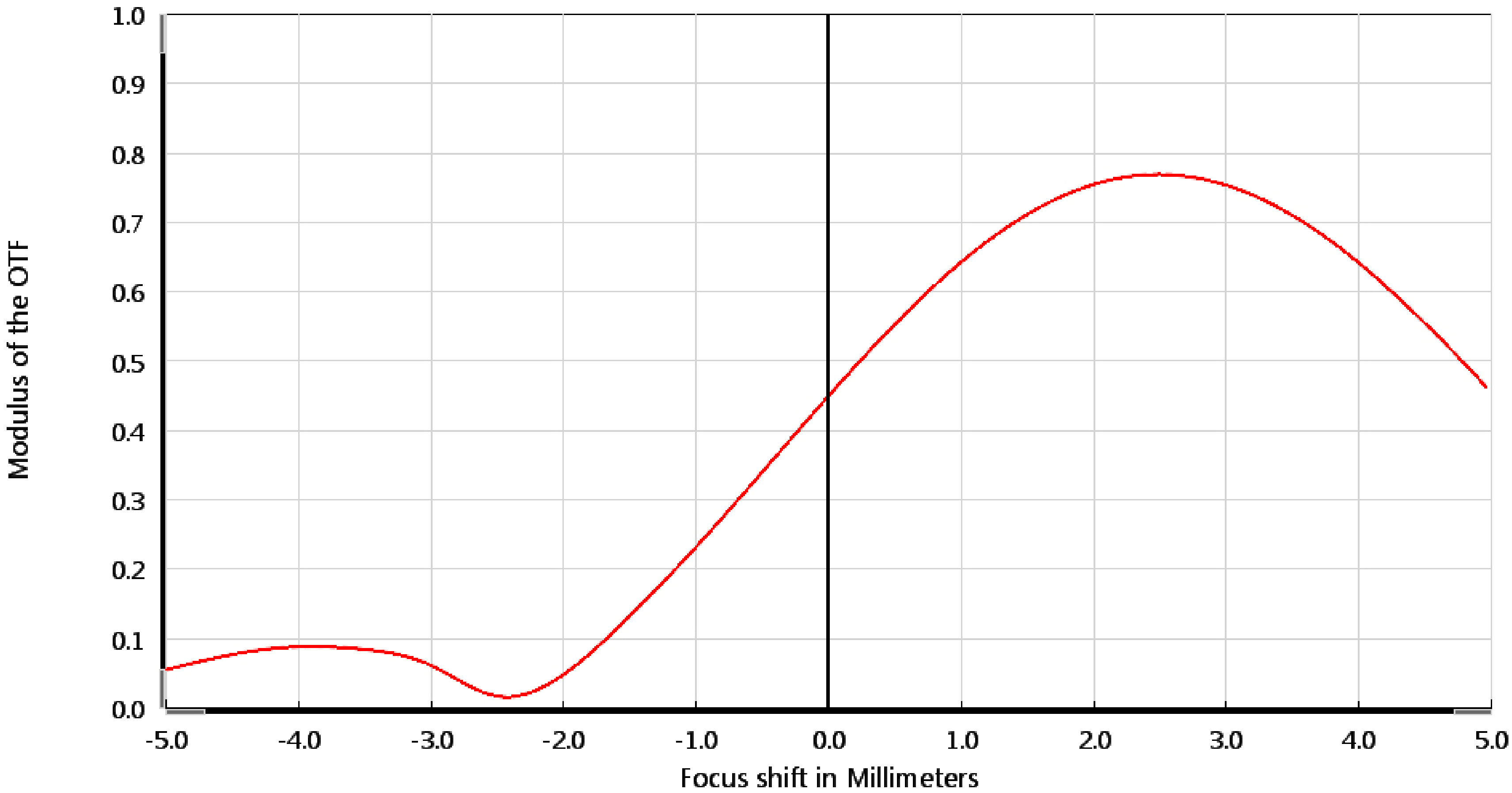

Figure 2-24 *The through-focus MTF of a simple lens system shows the MTF at a particular frequency (here, at 10 cycles/mm) over a range of focal plane locations, focus shifts from -5.0 to +5.0 mm. It is apparent that the modulation peaks for a focus shift that is approximately 2.5 mm from the nominal focal position.*